Apolar Polyisoprenoids Located in the Midplane of the Bilayer Regulate the Response of an Archaeal-like Membrane to High Temperature and Pressure

Josephine G Loricco, Marta Salvador-Castell, Bruno Demé, Judith Peters, Philippe Oger

Apolar Polyisoprenoids Located in the Midplane of the Bilayer Regulate the Response of an Archaeal-like Membrane to High Temperature and Pressure

Josephine G. Loricco[1, 2], Marta Salvador-Castell[2, 1], Bruno Demé[3], Judith Peters[3, 4, 5*], Philippe M. Oger[1, 2*]

[1]UMR5240 Microbiologie, Adaptation et Pathogenie (MAP), France, [2]Institut National des Sciences Appliquées de Lyon (INSA Lyon), France, [3]Institut Laue-Langevin, France, [4]Université Grenoble Alpes, France, [5]UMR5588 Laboratoire Interdisciplinaire de Physique (LIPhy), France

Submitted to Journal:
Frontiers in Chemistry

Specialty Section:
Physical Chemistry and Chemical Physics

Article type:
Original Research Article

Manuscript ID:
594039

Received on:
12 Aug 2020

Revised on:
30 Sep 2020

Frontiers website link:
www.frontiersin.org

Conflict of interest statement

The authors declare that the research was conducted in the absence of any commercial or financial relationships that could be construed as a potential conflict of interest

Author contribution statement

PO, MS, and JP conceived the project. MS, BD, JP, and PO carried out the experiments. JL performed the data analysis and wrote the initial draft. All authors contributed to the final manuscript.

Keywords

Archaea, Archaeal lipids, high pressure, Phase coexistence, membrane architecture, adaptation, membrane

Abstract

Word count: 189

Archaea are known to inhabit some of the most extreme environments on Earth. The ability of archaea possessing membrane bilayers to adapt to high temperature (>85°C) and high pressure (>1000 bar) environments is proposed to be due to the presence of apolar polyisoprenoids at the midplane of the bilayer. In this work, we study the response of this novel membrane architecture to both high temperature and high hydrostatic pressure using neutron diffraction. A mixture of two diether, phytanyl chain lipids (DoPhPC and DoPhPE) and squalane was used to model this novel architecture. Diffraction data indicate that at high temperatures a stable coexistence of fluid lamellar phases exists within the membrane and that stable coexistence of these phases is also possible at high pressure. Increasing the amount of squalane in the membrane regulates the phase separation with respect to both temperature and pressure, and also leads to an increase in the lamellar repeat spacing of both phases. The ability of squalane to regulate the ultrastructure of an archaea-like membrane at high pressure and temperature supports the hypothesis that archaea can use apolar lipids as an adaptive mechanism to extreme conditions.

Contribution to the field

We provide an exhaustive characterization of a model membrane with a novel membrane bilayer ultrastructure which midplane is populated by apolar polyisoprenoids. Physical parameters were determined from neutron diffraction on multilayered ordered stacks of reconstructed membranes, in presence or absence of the apolar lipids. We characterized the localization of the apolar molecule, the order parameters, size, shape and domain formation of the lipid membranes. We confirm the predicted presence of the apolar polyisporenoid molecules whithin the bilayer midplane, and validate the shift of the stability domain of the bilayer to higher temperatures and pressures. The lipid system is present as a coexistence of two lamellar phases. The apolar intercalant allows the switch between the two phases as a function of P and T. We demonstrate that the presence of the apolar molecules increase membrane properties and stability shifting the biologically relevant, functional, domain significantly to consider the quantity of apolar intercalant inside the midplane of the bilayer as an adaptative route of extremophiles to thrive under extreme P and T conditions. These results are directly transposable to articifial membrane systems to increase membrane/liposomes stability without increase costs since it would not require the synthesis of ipolar, membrane spanning lipids.

Funding statement

French National Research Agency programme ANR 17-CE11-0012-01

Ethics statements

Studies involving animal subjects
Generated Statement: No animal studies are presented in this manuscript.

Studies involving human subjects
Generated Statement: No human studies are presented in this manuscript.

Inclusion of identifiable human data
Generated Statement: No potentially identifiable human images or data is presented in this study.

Data availability statement

Generated Statement: The datasets presented in this study can be found in online repositories. The names of the repository/repositories and accession number(s) can be found below: http://dx.doi.org/10.5291/ILL-DATA.8-02-852.

Apolar Polyisoprenoids Located in the Midplane of the Bilayer Regulate the Response of an Archaeal-like Membrane to High Temperature and Pressure

Josephine G. LoRicco[1], Marta Salvador-Castell[1,#], Bruno Demé[2], Judith Peters[2,3,*], Philippe M. Oger[1*]

[1]Univ Lyon, INSA de Lyon, CNRS, MAP UMR 5240, Villeurbanne, France.

[2]Institut Laue-Langevin, F-38000 Grenoble, France.

[3]Université Grenoble Alpes, LiPhy, F-38044 Grenoble, France.

*** Correspondence:**
Philippe M. Oger
philippe.oger@insa-lyon.fr

Judith Peters
peters@ill.fr

[#]Current address: University of California San Diego, La Jolla, CA 92093-0319, USA.

Keywords: Archaea, archaeal lipids, high pressure, phase coexistence, membrane architecture, adaptation

Abstract

Archaea are known to inhabit some of the most extreme environments on Earth. The ability of archaea possessing membrane bilayers to adapt to high temperature (>85°C) and high pressure (>1000 bar) environments is proposed to be due to the presence of apolar polyisoprenoids at the midplane of the bilayer. In this work, we study the response of this novel membrane architecture to both high temperature and high hydrostatic pressure using neutron diffraction. A mixture of two diether, phytanyl chain lipids (DoPhPC and DoPhPE) and squalane was used to model this novel architecture. Diffraction data indicate that at high temperatures a stable coexistence of fluid lamellar phases exists within the membrane and that stable coexistence of these phases is also possible at high pressure. Increasing the amount of squalane in the membrane regulates the phase separation with respect to both temperature and pressure, and also leads to an increase in the lamellar repeat spacing of both phases. The ability of squalane to regulate the ultrastructure of an archaea-like membrane at high pressure and temperature supports the hypothesis that archaea can use apolar lipids as an adaptive mechanism to extreme conditions.

1 Introduction

According to the Singer-Nicolson model, cell membranes are composed of a "mosaic" of proteins embedded in a fluid, lipid bilayer (Singer and Nicolson, 1972). Our understanding of cell membranes has developed further since then, for example we now recognize the importance of other lipid phases in addition to the fluid lamellar phase (bilayer phase), and that there can be substantial lateral heterogeneity within the membrane (Goñi, 2014). Membrane structural lipids, typically phospholipids, are diverse and display varied properties owing to the differences in both the lipid polar head groups and the hydrophobic tails. In aqueous solution, these lipids, driven by the hydrophobic effect, self-assemble into structures in which the hydrophilic heads can interact with the solution and the hydrophobic tails are excluded. The most biologically common phases, seen in familiar lipid bilayer structures, are lamellar phases in which the lipids assemble into flat sheets (zero membrane curvature) (Cullis et al., 1991; Perutková et al., 2009; Frolov et al., 2011; Goñi, 2014). However, the ability of membrane to form phases with non-zero curvature, such as cubic or inverted hexagonal phases, is also important and plays a role in many cellular processes such as membrane fission and fusion (Jouhet, 2013; McMahon and Boucrot, 2015; Jarsch et al., 2016). Membrane lipids can prefer different membrane curvatures based on their shape, and this preferred curvature can vary with environmental conditions such as pressure and temperature. The presence of diverse lipids within a membrane can even promote phase separation and domain formation within the membrane (Jouhet, 2013). Domains are laterally organized membrane regions with distinct lipid compositions and specialized functions such as interacting with specific proteins, or adopting a specific curvature (Tayebi et al., 2012; Arumugam and Bassereau, 2015; Marquardt et al., 2015). Such lateral membrane domains have been well-characterized in eukaryotic and bacterial cells (Baumgart et al., 2003; Heberle and Feigenson, 2011; Heberle et al., 2013; McCarthy et al., 2015; Schmid, 2017).

Life has been found at some of the most extreme conditions on Earth such as temperatures above 100°C and pressures up to 120 MPa (Yayanos et al., 1981; Takai et al., 2008; Zeng et al., 2009; Dalmasso et al., 2016; Siliakus et al., 2017). All aspects of these organisms must be specially adapted to tolerate such conditions. Cell membranes, in particular, are highly sensitive to pressure and temperature (Winter and Jeworrek, 2009; Oger and Jebbar, 2010; Brooks and Seddon, 2014). In order to maintain functionality of the membrane under extreme conditions cells adjust the composition of their membranes to cope with environmental changes, in a process known as homeoviscous adaptation (Sinensky, 1974). High temperature tends to increase membrane fluidity, permeability, and promote more negative membrane curvature whereas increasing pressure tends to have the opposite effects (Brooks, 2014). To compensate, bacteria and eukaryotes are known to regulate the length, saturation, and branching of the hydrophobic chains as well as the proportion of different polar headgroups (Jebbar et al., 2015; Siliakus et al., 2017). In archaea the mechanisms of adaptation are less well understood, in part due to their unique membrane lipids. Archaeal lipids have methyl-branched phytanyl chains rather than straight chain fatty acids which are linked via ether rather than ester bonds to the glycerol backbone (De Rosa et al., 1986; Gambacorta et al., 1995). These lipids have higher temperature stability, and lowered proton permeability (Gliozzi et al., 1983; Yamauchi et al., 1993) compared with typical bacterial/eukaryotic lipids.

In addition to bilayer forming lipids, archaea are known to produce bipolar, tetra-ether lipids capable of forming lipid monolayers with high stability and low permeability (De Rosa et al., 1983; Elferink et al., 1994). Archaea have been shown to increase the quantity of tetra-ether lipids in the membrane in response to temperature (Matsuno et al., 2009; Cario et al., 2015). Even some bacteria have shown to produce membrane spanning tetraether or tetraester lipids in response to high-temperature conditions (Damsté et al., 2007; Schouten et al., 2007; Siliakus et al., 2017). Despite the link to high temperature adaption, tetra-ether lipids are not found solely in thermophiles but have also

been observed in mesophilic archaea. In addition, not all organisms living at high temperatures produce large quantities, if any tetra-ether lipids (Tornabene and Langworthy, 1979; Hafenbradl et al., 1996; Sako et al., 1996; Sprott et al., 1997; Siliakus et al., 2017). Some insight into the ability of archaea with bilayer forming lipids to live at temperatures up to 100°C can be found in the study by Cario et al. (2015) on the piezo-hyperthermophilic archaeon, *Thermococcus barophilus*. The quantity and saturation of isoprenoid derivatives (such as lycopane, squalane) were shown to vary in response to temperature and pressure. In order to explain the ability of *T. barophilus* to live at high temperature in presence of bilayer forming lipids, it was hypothesized that apolar lipids sit at the midplane of the bilayer and provide enhanced stability (Cario et al., 2015). The ability of apolar lipids such as squalane to localize to the midplane of the lipid bilayer has been confirmed in model membranes of both bacterial-like and archaea-like lipids (Hauß et al., 2002; Salvador-Castell et al., 2020b). The presence of apolar molecules is capable of modulating membrane physicochemical properties, for example, the presence of squalane at the bilayer midplane has been shown to increase permeability to water and decrease proton permeability (Haines, 2001). Apolar molecules at the midplane have been shown to increase the tendency towards negative membrane curvature by reducing packing frustration (Salvador-Castell et al., 2020b, 2020a) and to play a role in phase separation and domain formation (Gilmore et al., 2013; Salvador-Castell et al., 2020b). Such isoprenoid hydrocarbons are found in all archaea (Langworthy et al., 1982) suggesting this hypothesis could be extended to explain adaptation to high temperature and pressure in other archaea processing lipid bilayers.

In this work we studied the behavior of an archaeal-like bilayer with the proposed novel architecture composed of 1,2-di-O-phytanyl-*sn*-glycero-3-phosphocholine (DoPhPC) and 1,2-di-O-phytanyl-*sn*-glycero-3-phosphoethanolamine (DoPhPE) and 2,6,10,15,19,23-hexamethyltetracosane (squalane) under high temperature and high pressure conditions, mimicking the extreme conditions in which some archaea live. Using neutron diffraction, we are able to see the localization of squalane in the midplane bilayer, and to detect the presence of coexisting lamellar phases within the membrane. The structure of each phase as well as the phase coexistence were shown to vary in response to temperature and pressure. The response of the membrane ultrastructure to temperature and pressure could be modulated by varying the quantity of the apolar lipid squalane present in the membrane.

2 Material and Methods

2.1 Chemicals

1,2-di-O-phytanyl-*sn*-glycero-3-phosphocholine (DoPhPC) and 1,2-di-O-phytanyl-*sn*-glycero-3-phosphoethanolamine (DoPhPE) were both purchased from Avanti Polar Lipids (Alabaster, USA) in the lyophilized form and utilized without further purification. The isoprenoid used, 2,6,10,15,19,23-hexamethyltetracosane (squalane) was bought from Sigma – Aldrich Co (Montana, USA) in its hydrogenated form and from CDN Isotopes (Pointe-Claire, Canada), in its deuterated form.

2.2 Sample Preparation

3 mg of DoPhPC:DoPhPE (9:1 molar) and the corresponding amount of either hydrogenated squalane (h-squalane) or deuterated squalane (d-squalane) were dissolved in chloroform:methanol (2:1) and were spread on a silicon wafer using the "rock and roll" method (Tristram-Nagle, 2007) and dried overnight under high vacuum. Next, the sample was hermetically sealed inside an aluminum sample holder containing a 1:1 ratio of H_2O:D_2O (50% D_2O). The sample was left at 50 °C for 48h to allow for complete hydration.

2.3 Neutron Diffraction

Neutron diffraction experiments were performed on D16 (Cristiglio et al., 2015) at the Institut Laue-Langevin (Grenoble, France). The incident wavelength was 4.52 Å. The accessible q-range was from 0.06 $Å^{-1}$ to 0.51 $Å^{-1}$. The H_2O/D_2O contrast was 50% D_2O. 50% D_2O was previously found to give both strong diffraction signal and good resolution between the first order peaks of the two lamellar phases. The temperature was carefully controlled by placing the sample holder in a cryostat. Samples were either measured in a high temperature (HT) sample holder or in a HT-high hydrostatic pressure (HHP) cell (Peters et al., 2018). Data obtained at ILL are identified by doi: 10.5291/ILL-DATA.8-02-852 (Salvador-Castell et al., 2018).

Data treatment was performed by LAMP (Richard et al., 1996) and Origin Pro (Version 2019, OriginLab Corperation, Northampton, MA, USA). The integrated intensities of the Bragg peaks were corrected according to the absorption and analyzed by a Gaussian function, as done previously (Salvador-Castell et al., 2020c). The angle (θ) of a Bragg peak is related to the scattering vector (q) by:

$$q = \frac{4\pi sin(\theta)}{\lambda} \quad (1)$$

where λ is the wavelength. In cases where many orders of diffraction were visible, a linear fit of the form y = a + bx was performed on a plot of peak location (q) vs. diffraction order (h). The slope of the line (Δq) was used to determine the d-spacing using the following equation:

$$d = \frac{2\pi}{\Delta q} \quad (2)$$

In cases where only a single Bragg order was visible, the d-spacing was calculated using the first order peak and corrected based on the y-intercept determined for each sample under conditions where multiple peaks were present.

To locate squalane in the membrane we used the method described in (Hauß et al., 2002, 2005) taking advantage of difference scattering density between hydrogen and deuterium. Neutron scattering length density (NSLD) profiles are constructed from the sum of the neutron scattering lengths per unit volume (Marquardt et al., 2015). The NSLD profiles were calculated from a discrete set of Fourier coefficients (F_h) using the following equation (Katsaras, 1995):

$$\rho(z) = \frac{2}{d}\sum_{h=1}^{h_{max}} |F_h| v_n cos\left(\frac{2h\pi}{d} z\right), \quad (3)$$

where d is the lamellar spacing of the bilayer in the z direction, $z \in \left[\frac{-d}{2}, \frac{d}{2}\right]$, $|F_h| = \pm\sqrt{I_h Q_z}$, Q_z is the Lorentz correction factor equal to q for oriented bilayers, I_n is the integrated intensity of the h^{th} Bragg peak and v_n is the phase of the structure factor. The assigned phases of structure factors 1 to 4 (-, +, +, -) were based on those previously determined for this (DoPhPC:DoPhPE(9:1) + squalane) (Salvador-Castell et al., 2020a).

3 Results and Discussion

3.1 Stable phases coexist within archaeal-like membrane at high temperature and pressure

Cario et al. (2015) proposed a novel membrane architecture to explain the stability of archaea lipid bilayers under high pressure and temperatures. In this novel membrane architecture, apolar lipids act as structural lipids, sitting at the midplane of the lipid bilayer and leading to enhanced membrane stability under extreme conditions (Oger and Cario, 2013; Cario et al., 2015; Salvador-Castell et al., 2020a). A synthetic archaeal-like membrane composed of a mixture of diphytanyl lipids (DoPhPC and

DoPhPE in a 9 to 1 molar ratio) and the apolar lipid squalane was used to model this novel architecture. The chemical structures of these lipids are shown in Figure S1. In order to probe how this membrane behaves under the extreme conditions of temperature and pressure faced by archaea, neutron diffraction was performed on oriented stacked bilayers at temperatures up to 85°C and pressures up to 1000 bar. Experiments were performed with both hydrogenated squalane (h-squalane) and deuterated squalane (d-squalane) in order to take advantage of the differential neutron scattering between hydrogen and deuterium (Hauß et al., 2002, 2005). The neutron scattering length density (NSLD) for membranes containing h-squalane and d-squalane was plotted as a function of distance (Figure S2). For convenience, 0 Å represents the midplane of the bilayer. These plots exhibit two characteristic maxima corresponding to the glycerol backbone and a minimal intensity near the terminal methyl groups. The spectra for the membrane containing h-squalane and d-squalane overlap fairly well except within the region corresponding to the midplane of the bilayer (-10 to 10 Å) where the sample containing d-squalane shows an excess of scattering density. This indicates that squalane is located in the midplane of the bilayer and is in agreement with the findings of Salvador-Castell et al. (2020b). In this work we see that this localization of squalane is seen in both $Phase_{LT}$ and $Phase_{HT}$ at low (20 bar) and high (1000 bar) pressure.

The stacked multilayers were sufficiently ordered in the membrane to give rise to Bragg peaks in the diffraction data. Figure 1A shows the 1D neutron diffraction profiles for a membrane composed of DoPhPC:DoPhPE (9:1) + 5 mol% h-squalane at 20 bar (black spectra). The temperature increased from 25°C (bottom) to 85°C (top). At 25°C, there were three orders of diffraction for the sample at low pressure (20 bar). The first order diffraction peak was located at q = ~0.12 $Å^{-1}$, the second order peak at q = ~0.23 $Å^{-1}$, and the third order peak at q = ~0.34 $Å^{-1}$. The location of peaks in the ratio of (1, 2, 3...) indicates a lamellar phase (Tyler et al., 2015). As the temperature increased, the peaks corresponding to the original phase were still present at similar values of q (marked with an 'x'), although with diminished intensities. At higher temperatures (above 40 °C) a second set of peaks appeared at lower values of q corresponding to a new phase (marked with an 'o'). The first order diffraction peak of this new phase is located at q = ~0.09 $Å^{-1}$ and the second order diffraction peak at q = ~0.18 $Å^{-1}$. The spacing of the peaks indicates that this new phase is also lamellar. We will refer to the new phase as $Phase_{HT}$ because it appeared at high temperatures (HT) compared to the original phase, which is also present at low temperatures (LT) and will therefore be referred to as $Phase_{LT}$. Increasing temperature leads to an increase in the intensity of the $Phase_{HT}$ peaks indicating that temperature stabilizes $Phase_{HT}$, and leads to a decrease in the intensity of $Phase_{LT}$ indicating that temperature destabilizes $Phase_{LT}$. Upon returning the membrane to 25 °C and 20 bar, the initial state, is restored indicating that this change in phase is fully reversible (Figure 1A).

At each temperature, the diffraction of the DoPhPC:DoPhPE (9:1) + 5 mol% h-squalane membrane was measured at 20, 250, 500, and 1000 bar. The Figure 1 insets show the first order diffraction peaks, indicated by the red boxes, seen at pressures of 20 bar (black), 250 bar (red), 500 bar (blue) and 1000 bar (green). At 85 °C and 55 °C, two first order diffraction peaks are seen, representing the two phases. The area of the $Phase_{HT}$ peak (found at lower q) decreases and the area of the $Phase_{LT}$ peak (found at higher q) increases as a function of pressure (Figure 1B, Figure 1C). This indicates that high pressure has a stabilizing effect on $Phase_{LT}$ and a destabilizing effect on $Phase_{HT}$. Although it is well-established that increasing pressure causes an effect similar to decreasing the temperature, our results show that even 1000 bar is not enough to completely replace $Phase_{HT}$ and return to the lipid organization present at lower temperatures. At 25 °C, the membrane is exclusively in $Phase_{LT}$. Again, there is a slight increase in the intensity of the $Phase_{LT}$ peak with pressure indicating that pressure stabilizes $Phase_{LT}$ (Figure 1D).

Both pressure and temperature play an important role in the stability of each phase and their ability to coexist. In order to better quantify the temperature and pressure range at which these phases coexist, the change in the integrated peak intensities was monitored as a function of temperature at each pressure (20, 250, 500 and 1000 bar). The changes in the peak intensities of the first order peaks of both $Phase_{LT}$ and $Phase_{HT}$ have a linear dependence on temperature (Figure 2 A-D, Figure S3). A linear fit could be used to extrapolate/interpolate when the peak intensity would be zero and thus to determine the temperature at which the corresponding phase was no longer present in the membrane for each pressure, as shown in Figure 2.

The integrated peak intensities of $Phase_{LT}$ (blue) and $Phase_{HT}$ (green) at 20 bar were analyzed as a function of temperature (Figure 2A). A linear fit of the integrated $Phase_{HT}$ peak intensities determined that the peak intensity would equal zero at 34.3 ± 3.9 °C, signifying that $Phase_{HT}$ appears above this temperature. Below this temperature, the membrane is exclusively in $Phase_{LT}$. A linear fit of the $Phase_{LT}$ peak intensities determined that the peak intensity would reach zero at 85.3 ± 1.2 °C. Above this temperature, $Phase_{LT}$ would disappear and the membrane would be entirely in $Phase_{HT}$. Between these two temperatures, both phases coexist. This analysis was repeated with the data taken at 250, 500, and 1000 bar (Figure 2 B-D), allowing the determination of a pressure-temperature diagram of the phase coexistence of $Phase_{LT}$ and $Phase_{HT}$ (Figure 2E). The temperature at which $Phase_{HT}$ appears (T_{HT}) increased with increasing pressure from 34.3 ± 3.9 °C at 20 bar to 37.4 ± 3.2 °C at 250 bar, 37.7 ± 3.0 °C at 500 bar and to 38.9 ± 2.6 °C at 1000 bar. The increase in T_{HT} with pressure was small (~5 °C/kbar) and was not statistically significant The temperature at which $Phase_{LT}$ disappeared (T_{LT}) also increased with increasing pressure from 85.3 ± 1.2 °C at 20 bar, to 90.2 ± 2.3 °C at 250 bar, 99.7 ± 5.7 °C at 500 bar and finally to 108.0 ± 6.9 °C at 1000 bar. The increase in T_{LT} as a function of pressure was much larger (~24 °C/kbar) (Figure 2E). Here we demonstrate that although the phases are pressure sensitive, phase coexistence is possible at pressures up to, and presumably above, 1000 bar. Based on the phase diagram, at high temperatures (> 85 °C), the application of pressure is predicted to induce phase separation from solely $Phase_{HT}$ at low pressure to a coexistence of $Phase_{HT}$ and $Phase_{LT}$ at high pressure and high temperature. Pressure induced phase separation is not a novel concept, as high pressure has been previously shown to be capable of inducing phase separation and domain formation (McCarthy et al., 2015). Our results suggest that this is also possible in membranes composed of archaeal lipids. It should be noted that the T_{HT} and T_{LT} reported here were calculated only as the sample being heated, and that the transition temperature upon cooling was not explicitly tracked. Membranes are known to exhibit hysteresis near phase transitions meaning that the transition temperatures upon heating and cooling are different. A similar effect has also been seen in membranes upon pressurization/depressurization (Trovaslet-Leroy et al. 2016).

From the changes in peak intensity, it could be determined that pressure destabilizes $Phase_{HT}$ and stabilizes $Phase_{LT}$. In addition to changes in the integrated intensities of the peaks, there were also changes in the location of the peaks with pressure that reflect changes in the lamellar repeat structure. The multilayer organization of the membranes makes it simple to determine the repeat spacing (d), which includes the thickness of the bilayer and its associated water layer (Nagle and Tristram-Nagle, 2000), from the location of the Bragg peaks of each phase. For a lamellar phase, the repeat spacing (d) can be calculated simply by equation (3), where q is the location of the first order lamellar peak. The d-spacing of both $Phase_{LT}$ (solid symbols) and $Phase_{HT}$ (open symbols) increase as a function of pressure (Figure 3A). The d-spacing of $Phase_{LT}$ with increasing pressure is shown again in Figure 3B using a different scale to better visualize the changes. $Phase_{LT}$ exhibits either a small increase or negligible change in d-spacing with increasing pressure. Linear fitting of the data determined that the d-spacing of $Phase_{LT}$ increases at a rate of 0.23 ± 0.32 Å/kbar at 25 °C, 0.61 ± 0.13 Å/kbar at 40 °C, 0.53 ± 0.11 at 55 °C, 0.09 ± 0.30 at 70 °C and 0.40 ± 0.16 at 85 °C. An increase in membrane d-spacing with pressure has been observed previously (Winter and Jeworrek, 2009; Trapp et al., 2013; Brooks

and Seddon, 2014). Increasing pressure provokes a lateral compression of membrane lipids and an increase in membrane thickness due to extension of the hydrocarbon chains. The d-spacing of $Phase_{HT}$ also increases with pressure (Figure 3A). The d-spacing increased at a rate of 5.84 ± 0.81 Å/kbar at 40 °C, 5.78 ± 0.19 Å/kbar at 55 °C, 3.91 ± 0.36 Å/kbar at 70 °C, and 2.62 ± 0.22 Å/kbar at 85 °C. The changes in d-spacing for $Phase_{HT}$ were almost an order of magnitude greater than that seen in $Phase_{LT}$ showing that $Phase_{HT}$ is much more sensitive to changes in pressure. It is interesting to note that the swelling of $Phase_{HT}$ decreases with temperature.

The formation of a new phase, $Phase_{HT}$, is most likely due to the presence of lipids with different preferred curvatures within the membrane as seen by Salvador-Castell et al., (2020b). The bilayer is made up of two phytanyl lipids with different polar head groups (DoPhPC and DoPhPE) and the apolar isoprenoid squalane. The phosphoethanolamine (PE) headgroup is small, so the lipid has a conical geometry and favors a negative curvature (favoring the formation of non-lamellar structure such as inverted hexagonal phases/cubic phases/inverted micelles). The phosphocholine (PC) headgroup is larger and the lipid has a cylindrical geometry which favors zero-curvature (favoring the formation of lamellar structures such as bilayers). The PC headgroup can stabilize the lamellar phase of PE lipids (Kates and Manson, 1984). The phase separation can be explained by partitioning of DoPhPC and DoPhPE into different phases based on preferred curvature which can be triggered, for example, by temperature which favors more negative membrane curvatures. The presence of squalane also promotes negative lipid curvature and was found to forward the formation of non-lamellar phases in a DoPhPC:DoPhPE (9:1) membrane (Salvador-Castell et al., 2020b, 2020a). Increasing pressure, on the other hand, tends to increase the preferred membrane curvature (Shearman et al., 2006; Brooks, 2014). In our model membrane, phase separation was triggered by increasing temperature, which could be due to the differences in curvature between the lipids becoming too great to remain within the same phase. Increasing pressure hinders the phase separation and favors $Phase_{LT}$, lending further support to the idea that the phase separation is driven by components of different curvature.

Increasing negative curvature favors a transition from a lamellar phase to a non-lamellar phase. Although no such phases were seen by neutron diffraction, non-lamellar phases in this membrane system have been detected by SAXS (Salvador-Castell et al., 2020a). Neutron scattering was performed on multi-stacks of bilayers on a silicon wafer, whereas for the SAXS the sample was not ordered on a substrate but rather was self-assembled in bulk. These differences in lipid preparation may explain why in one case the DoPhPC:DoPhPE (9:1) + 5 mol% squalane membrane separates into two lamellar phases and in the other case the membrane separates into a lamellar phase and an inverted hexagonal phase. The ordering of the lipids on a solid support for neutron diffraction may impede the formation of non-lamellar phases. For both phases seen by neutron diffraction, increasing pressure leads to an increase in the membrane d-spacing, however, the magnitude of the pressure-induced swelling was significantly different between the phases. The changes in $Phase_{LT}$ are small, generally within the error of the measurements for the d-spacing. The changes in $Phase_{HT}$ are quite large (2-6 Å/kbar). The pressure-induced swelling of the $Phase_{HT}$ seen by neutron diffraction is unusually large for a lamellar phase which is typically < 2 Å/kbar (Brooks, 2014). Interestingly, the magnitude of the pressure-induced swelling seen in $Phase_{HT}$ is similar to that seen in the inverted hexagonal phase seen by SAXS (Salvador-Castell et al., 2020a). Figure S4 illustrates how the membrane lattice parameter (equal to d for lamellar phase and 2/3 d for inverted hexagonal phase) increases as a function of pressure. The similarities in the response to pressure of $Phase_{HT}$ and the inverted hexagonal phase seen in SAXS could be due to the partitioning of lipid headgroups and squalane in a similar manner.

3.2 Squalane regulates membrane ultrastructure under high temperature and pressure

Archaea are thought to regulate their membranes response to extreme conditions with apolar lipids. For this reason, the neutron diffraction experiments were repeated with two additional concentrations of hydrogenated squalane, 2.5 mol% and 10 mol% in order to determine what effect the amount of squalane would have on the membrane structure at high temperatures and pressures. Two coexisting phases are also present in membranes containing 2.5 mol% or 10 mol% squalane at elevated temperatures (Figure S5, Figure S6).

The repeat spacing of $Phase_{LT}$ and $Phase_{HT}$ was calculated for the membranes containing 2.5 mol%, 5 mol% and 10 mol% squalane and the values are displayed in Table 1. In all membranes, there is an increase in the membrane d-spacing with increasing pressure, and $Phase_{HT}$ is again found to be the more pressure-sensitive phase (Figure 4). The pressure induced swelling of $Phase_{LT}$ remains small ($\leq$ 1Å/kbar) for all squalane concentrations and is not significantly different with changes in temperature. The pressure induced swelling of $Phase_{HT}$ is much larger (2-8 Å/kbar) and the swelling of $Phase_{HT}$ is temperature dependent. The swelling is significantly larger at low temperatures and smaller at high temperatures. Although the percentage of squalane does not change the swelling of $Phase_{HT}$, the amount of squalane does play an important role in affecting the temperature range at which $Phase_{HT}$ is present. At $\geq$ 55 °C, $Phase_{HT}$ is seen in membranes containing 2.5 mol%, 5 mol% and 10 mol% squalane. At 40°C, $Phase_{HT}$ is no longer capable of forming the membrane containing 2.5 mol% squalane and at 25°C, $Phase_{HT}$ is only seen in the membrane containing 10 mol% squalane.

The temperatures at which $Phase_{HT}$ appears for a membrane containing either 2.5 mol% or 10 mol% squalane are determined from a linear fit of integrated peak intensity vs temperature (Figure S3). As seen previously with the membrane containing 5 mol% squalane, pressure leads to an increase in T_{HT} and T_{LT} (Figure S7). Increasing the quantity of squalane promotes the formation of $Phase_{HT}$ at lower temperatures. For example, at 20 bar $Phase_{HT}$ appears at 44.7 ± 4.0 °C for the membrane containing 2.5 mol% squalane, 34.3 ± 3.9 °C for the membrane containing 5 mol% squalane and 23.9 ± 3.4 °C for the membrane containing 10 mol% squalane. The concentration of squalane has a similar effect on T_{HT} at elevated pressures (Table 2).

This agrees with previous findings that squalane promotes negative membrane curvature, favoring the formation of $Phase_{HT}$ and phase separation at lower temperatures (Salvador-Castell et al., 2020a, 2020b). Here we show that squalane is also capable of promoting the formation of $Phase_{HT}$ at high pressures. Previously at ambient pressure, it was shown that the phase coexistence and lateral organization within a DoPhPC:DoPhPE membrane was squalane dependent leading to the hypothesis that squalane may promote the formation of membrane domains (Salvador-Castell et al., 2020b). That would mean that the ability of squalane to favor phase separation at high pressures, may indicate that squalane could also promote domain formation in archaea that live at such high-pressure conditions.

In addition to regulating the phase coexistence within the membrane, increasing the amount of squalane in the membrane also affects the d-spacing. The d-spacing of the membrane is typically higher when the membrane contains a higher quantity of squalane for $Phase_{HT}$ (Table 1, Figure S8). For example, in $Phase_{HT}$ at 20bar/55°C the d-spacing is 67.1Å when the membrane contains 2.5 mol% squalane compared with 68.1Å when the membrane contains 5 mol% squalane and 74.7 Å when the membrane contains 10 mol% squalane. In this experiment, we did not see a significant change in the d-spacing of $Phase_{LT}$ with increasing squalane concentration which was seen previously, at ambient pressure and temperature (Salvador-Castell et al., 2020b). The increase in d-spacing with increasing squalane for $Phase_{LT}$ was only seen up to 5 mol% squalane at which point the phase is thought to reach saturation. It is conceivable that the amount of squalane required to reach saturation within membrane could change with pressure and temperature and this may be one of the reason we did not see any change in the d-spacing of $Phase_{LT}$ with increasing squalane in this experiment.

At temperatures at which $Phase_{HT}$ was present, $Phase_{HT}$ was always found to increase in d-spacing with increasing squalane. Previously it was shown that increasing the percentage of squalane leads to an increase in the d-spacing in $Phase_{LT}$ due to an increase in the hydrophobic core thickness (Salvador-Castell et al., 2020b). The localization of squalane to the midplane of the bilayer is confirmed for $Phase_{HT}$ as well as $Phase_{LT}$ (Figure S2). This could indicate that the increase in the d-spacing for $Phase_{HT}$ is also due to an increase in hydrophobic core thickness although this cannot be directly confirmed from this data. Increasing squalane promotes changes in membrane structure of both phases, even at high pressures and temperatures, indicating that squalane could act as a membrane regulator under the extreme conditions at which many archaea live.

4 Conclusions

It was proposed by Cario et al., (2015) that apolar lipids, such as squalane, sit at the midplane of the lipid bilayer, and provide a means of enhancing the stability of archaeal membrane bilayers under extreme conditions. This localization of apolar lipids to the midplane of an archaeal-like bilayer was then confirmed by the work of Salvador-Castell et al, (2020b). The aims of this study were to determine how an archaeal-like membrane with this novel membrane architecture behaves in response to the high temperatures and high hydrostatic pressures and to determine how the quantity of apolar lipid present in the membrane modulates this behavior. To model the proposed membrane architecture in which apolar molecules sit in the midplane of the bilayer, we used an artificial archaea-like membrane composed of DoPhPC, DoPhPE and squalane. The use of neutron diffraction allowed us to confirm the localization of the apolar lipid squalane and to further study the coexistence of two distinct lamellar phases previously reported by Salvador-Castell et al., (2020b). The phase separation within the membrane is most likely due to the partitioning of lipids (DoPhPC/DoPhPE) with different preferred curvatures and the presence of the apolar molecule (squalane). The two phases are capable of coexisting at a wide range of temperatures and pressure. High temperature favors the formation of a swollen lamellar phase ($Phase_{HT}$) and high pressure favors a thinner lamellar phase ($Phase_{LT}$). The temperature and pressure range of the phase coexistence is regulated by the percentage of squalane present in the membrane. Increasing the percentage of squalane favors the formation of $Phase_{HT}$ at lower temperatures, for pressures up to 1000 bar. Coexistence and lateral organization of these phases was seen previously at ambient pressure (Salvador-Castell et al., 2020b). Here we have shown that phase coexistence is also seen at high pressure which could indicate the possibility of domain formation in archaea living at high pressure in addition to high temperature. Increasing the amount of squalane also leads to an increase in the membrane lamellar repeat spacing for $Phase_{HT}$. The ability of squalane to modify the membrane ultrastructure at both high pressure and temperature supports the hypothesis that apolar lipids play a role in adaptation of archaea to extreme conditions.

5 Conflict of Interest

The authors declare that the research was conducted in the absence of any commercial or financial relationships that could be construed as a potential conflict of interest.

6 Author Contributions

PO, MS, and JP conceived the project. MS, BD, JP, and PO carried out the experiments. JL performed the data analysis and wrote the initial draft. All authors contributed to the final manuscript.

7 Funding

This work was supported by the French National Research Agency programme ANR 17-CE11-0012-01 to PO and JP. MS was supported by a PhD grant from the French Ministry of Research.

8 Acknowledgments

The authors thank the Institut Laue-Langevin for the allocation of beamtime (doi: 10.5291/ILL-DATA.8-02-852) and for technical support with the high temperature and pressure setup.

1 Data Availability Statement

The raw data supporting the conclusions of this article will be made available by the authors, without undue reservation.

9 References

Arumugam, S., and Bassereau, P. (2015). Membrane nanodomains: Contribution of curvature and interaction with proteins and cytoskeleton. *Essays Biochem.* 57, 109–119. doi:10.1042/BSE0570109.

Baumgart, T., Hess, S. T., and Webb, W. W. (2003). Imaging coexisting fluid domains in biomembrane models coupling curvature and line tension. *Nature* 425, 821–824. doi:10.1038/nature02013.

Brooks, N. J. (2014). Pressure effects on lipids and bio-membrane assemblies. *IUCrJ* 1, 470–477. doi:10.1107/S2052252514019551.

Brooks, N. J., and Seddon, J. M. (2014). High pressure x-ray studies of lipid membranes and lipid phase transitions. *Zeitschrift fur Phys. Chemie* 228, 987–1004. doi:10.1515/zpch-2014-0602.

Cario, A., Grossi, V., Schaeffer, P., and Oger, P. M. (2015). Membrane homeoviscous adaptation in the piezo-hyperthermophilic archaeon Thermococcus barophilus. *Front. Microbiol.* 6. doi:10.3389/fmicb.2015.01152.

Cristiglio, V., Giroud, B., Didier, L., and Demé, B. (2015). D16 is back to business: more neutrons, more space, more fun. *Neutron News*, 22–24. doi:10.1080/10448632.2015.1057051.

Cullis, P. R., Tilcock, C. P., and Hope, M. J. (1991). "Lipid Polymorphism," in *Membrane Fusion*, eds. J. Wilschut and D. Hoekstra (CRC Press), 35–64.

Dalmasso, C., Oger, P., Courtine, D., Georges, M., Takai, K., Maignien, L., et al. (2016). Complete genome sequence of the hyperthermophilic and piezophilic archeon Thermococcus piezophilus CDGST, able to grow under extreme hydrostatic pressures. *Genome Announc.* 4, e00610-16. doi:10.1128/genomeA.00610-16.

Damsté, J. S. S., Rijpstra, W. I. C., Hopmans, E. C., Schouten, S., Balk, M., and Stams, A. J. M. (2007). Structural characterization of diabolic acid-based tetraester, tetraether and mixed ether/ester, membrane-spanning lipids of bacteria from the order Thermotogales. *Arch. Microbiol.* 188, 629–641. doi:10.1007/s00203-007-0284-z.

De Rosa, M., Gambacorta, A., and Gliozzi, A. (1986). Structure, biosynthesis, and physicochemical properties of archaebacterial lipids. *Microbiol. Rev.* 50, 70–80. doi:10.1128/mmbr.50.1.70-

425 80.1986.

426 De Rosa, M., Gambacorta, A., and Nicolaus, B. (1983). A new type of cell membrane, in
427 thermophilic archaebacteria, based on bipolar ether lipids. *J. Memb. Sci.* 16, 287–294.
428 doi:10.1016/S0376-7388(00)81316-2.

429 Elferink, M. G. L., De Wit, J. G., Driessen, A. J. M., and Konings, W. N. (1994). Stability and
430 proton-permeability of liposomes composed of archaeal tetraether lipids. *Biochim. Biophys.*
431 *Acta* 1193, 247–254. doi:10.1016/0005-2736(94)90160-0.

432 Frolov, V. A., Shnyrova, A. V., and Zimmerberg, J. (2011). Lipid polymorphisms and membrane
433 shape. *Cold Spring Harb. Perspect. Biol.* 3, a004747. doi:10.1101/cshperspect.a004747.

434 Gambacorta, A., Gliozzi, A., and De Rosa, M. (1995). Archaeal lipids and their biotechnological
435 applications. *World J. Microbiol. Biotechnol.* 11, 115–131. doi:10.1007/BF00339140.

436 Gilmore, S. F., Yao, A. I., Tietel, Z., Kind, T., Facciotti, M. T., and Parikh, A. N. (2013). Role of
437 squalene in the organization of monolayers derived from lipid extracts of halobacterium
438 salinarum. *Langmuir* 29, 7922–7930. doi:10.1021/la401412t.

439 Gliozzi, A., Paoli Mario Rosa, G. DE, and Gambacorta, A. (1983). Effect of isoprenoid cyclization
440 on the transition temperature of lipids in thermophilic archaebacteria. *Biochem. Biophys. acta*
441 735, 234–242. doi:10.1016/0005-2736(83)90298-5.

442 Goñi, F. M. (2014). The basic structure and dynamics of cell membranes: An update of the Singer-
443 Nicolson model. *Biochim. Biophys. Acta - Biomembr.* 1838, 1467–1476.
444 doi:10.1016/j.bbamem.2014.01.006.

445 Hafenbradl, D., Keller, M., and Stetter, K. O. (1996). Lipid analysis of Methanopyrus kandleri.
446 *FEMS Microbiol. Lett.* 136, 199–202. doi:10.1016/0378-1097(96)84201-7.

447 Haines, T. H. (2001). Do sterols reduce proton and sodium leaks through lipid bilayers? *Prog. Lipid*
448 *Res.* 40, 299–324. doi:10.1016/s0163-7827(01)00009-1.

449 Hauß, T., Dante, S., Dencher, N. A., and Haines, T. H. (2002). Squalane is in the midplane of the
450 lipid bilayer: implications for its function as a proton permeability barrier. *Biochem. Biophys.*
451 *acta* 1556, 149–54. doi:10.1016/s0005-2728(02)00346-8.

452 Hauß, T., Dante, S., Haines, T. H., and Dencher, N. A. (2005). Localization of coenzyme Q10 in the
453 center of a deuterated lipid membrane by neutron diffraction. *Biochim. Biophys. Acta -*
454 *Bioenerg.* 1710, 57–62. doi:10.1016/j.bbabio.2005.08.007.

455 Heberle, F. A., and Feigenson, G. W. (2011). Phase separation in lipid membranes. *Cold Spring*
456 *Harb. Perspect. Biol.* 3, 1–13. doi:10.1101/cshperspect.a004630.

457 Heberle, F. A., Petruzielo, R. S., Pan, J., Drazba, P., Kučerka, N., Standaert, R. F., et al. (2013).
458 Bilayer thickness mismatch controls domain size in model membranes. *J. Am. Chem. Soc.* 135,
459 6853–6859. doi:10.1021/ja3113615.

460 Jarsch, I. K., Daste, F., and Gallop, J. L. (2016). Membrane curvature in cell biology: An integration

of molecular mechanisms. *J. Cell Biol.* 214, 375–387. doi:10.1083/jcb.201604003.

Jebbar, M., Franzetti, B., Girard, E., and Oger, P. (2015). Microbial diversity and adaptation to high hydrostatic pressure in deep-sea hydrothermal vents prokaryotes. *Extremophiles* 19, 721–740. doi:10.1007/s00792-015-0760-3.

Jouhet, J. (2013). Importance of the hexagonal lipid phase in biological membrane organization. *Front. Plant Sci.* 4. doi:10.3389/fpls.2013.00494.

Kates, M., and Manson, L. A. (1984). *Membrane Fluidity*. New York: Plenum Press doi:10.1007/978-1-4684-4667-8.

Katsaras, J. (1995). X-ray diffraction studies of oriented lipid bilayers. *Biochem. Cell Biol.* 73, 209–218. doi:10.1139/o95-025.

Langworthy, T. A., Tornabene, T. G., and Holzer, G. (1982). Lipids of Archaebacteria. *Zent. Fur Bakteriol. Angew. Und Okol. Microbiol. Abt. L. Orig. C. Hyg.* 3, 228–244. doi:10.1016/S0721-9571(82)80036-7.

Marquardt, D., Heberle, F. A., Nickels, J. D., Pabst, G., and Katsaras, J. (2015). On scattered waves and lipid domains: Detecting membrane rafts with X-rays and neutrons. *Soft Matter* 11, 9055–9072. doi:10.1039/c5sm01807b.

Matsuno, Y., Sugai, A., Higashibata, H., Fukuda, W., Ueda, K., Uda, I., et al. (2009). Effect of growth temperature and growth phase on the lipid composition of the archaeal membrane from Thermococcus kodakaraensis. *Biosci. Biotechnol. Biochem.* 73, 104–108. doi:10.1271/bbb.80520.

McCarthy, N. L. C., Ces, O., Law, R. V., Seddon, J. M., and Brooks, N. J. (2015). Separation of liquid domains in model membranes induced with high hydrostatic pressure. *Chem. Commun.* 51, 8675–8678. doi:10.1039/c5cc02134k.

McMahon, H. T., and Boucrot, E. (2015). Membrane curvature at a glance. *J. Cell Sci.* 128, 1065–1070. doi:10.1242/jcs.114454.

Nagle, J. F., and Tristram-Nagle, S. (2000). Structure of lipid bilayers. *Biochim. Biophys. Acta* 1469, 159–195. doi:10.1016/s0304-4157(00)00016-2.

Oger, P. M., and Cario, A. (2013). Adaptation of the membrane in Archaea. *Biophys. Chem.* 183, 42–56. doi:10.1016/j.bpc.2013.06.020.

Oger, P. M., and Jebbar, M. (2010). The many ways of coping with pressure. *Res. Microbiol.* 161, 799–809. doi:10.1016/j.resmic.2010.09.017.

Perutková, Š., Daniel, M., Dolinar, G., Rappolt, M., Kralj-Iglič, V., and Iglič, A. (2009). "Stability of the Inverted Hexagonal Phase," in *Advances in Planar Lipid Bilayers and Liposomes*, 237–278. doi:10.1016/S1554-4516(09)09009-7.

Peters, J., Golub, M., Demé, B., Gonthier, J., Maurice, J., Payre, C., et al. (2018). New pressure cells for membrane layers and systems in solutions up to 100°C. *J. Neutron Res.* 20, 1–10.

doi:10.3233/JNR-180055.

Richard, D., Ferrand, M., and Kearley, G. J. (1996). Analysis and visualisation of neutron-scattering data. *J. Neutron Res.* 4, 33–39. doi:10.1080/10238169608200065.

Sako, Y., Nomura, N., Uchida, A., Ishida, Y., Morii, H., Koga, Y., et al. (1996). Aeropyrum pernix gen. nov., sp. nov., a novel aerobic hyperthermophilic archaeon growing at temperatures up to 100°C. *Int. J. Syst. Bacteriol.* 46, 1070–1077. doi:10.1099/00207713-46-4-1070.

Salvador-Castell, M., Brooks, N. J., Peters, J., and Oger, P. (2020a). Induction of non-lamellar phases in archaeal lipids at high temperature and high hydrostatic pressure by apolar polyisoprenoids. *Biochim. Biophys. Acta - Biomembr.* 1862. doi:10.1016/j.bbamem.2019.183130.

Salvador-Castell, M., Demé, B., Oger, P., and Peters, J. (2020b). Lipid phase separation induced by the apolar polyisoprenoid squalane demonstrates its role in membrane domain formation in archaeal membranes. *Langmuir*, 7375–7382. doi:10.1021/acs.langmuir.0c00901.

Salvador-Castell, M., Demé, B., Oger, P., and Peters, J. (2020c). Structural characterization of an archaeal lipid bilayer as a function of hydration and temperature. *Int. J. Mol. Sci.* 21. doi:10.3390/ijms21051816.

Salvador-Castell, M., Misuraca, L., Oger, P. M., and Peters, J. (2018). Novel high-pressure/high-temperature phases in archaeal membranes. doi:10.5291/ILL-DATA.8-02-852.

Schmid, F. (2017). Physical mechanisms of micro- and nanodomain formation in multicomponent lipid membranes. *Biochim. Biophys. Acta* 1859, 509–528. doi:10.1016/j.bbamem.2016.10.021.

Schouten, S., Van Der Meer, M. T. J., Hopmans, E. C., Rijpstra, W. I. C., Reysenbach, A. L., Ward, D. M., et al. (2007). Archaeal and bacterial glycerol dialkyl glycerol tetraether lipids in hot springs of Yellowstone National Park. *Appl. Environ. Microbiol.* 73, 6181–6191. doi:10.1128/AEM.00630-07.

Shearman, G. C., Ces, O., Templer, R. H., and Seddon, J. M. (2006). Inverse lyotropic phases of lipids and membrane curvature. *J. Phys. Condens. Matter* 18. doi:10.1088/0953-8984/18/28/S01.

Siliakus, M. F., van der Oost, J., and Kengen, S. W. M. (2017). Adaptations of archaeal and bacterial membranes to variations in temperature, pH and pressure. *Extremophiles* 21, 651–670. doi:10.1007/s00792-017-0939-x.

Sinensky, M. (1974). Homeoviscous adaptation: a homeostatic process that regulates the viscosity of membrane lipids in Escherichia coli. *Proc. Natl. Acad. Sci. U. S. A.* 71, 522–525. doi:10.1073/pnas.71.2.522.

Singer, S. J., and Nicolson, G. L. (1972). The fluid mosaic model of the structure of cell membranes. *Science* 175, 720–731. doi:10.1126/science.175.4023.720.

Sprott, G. D., Agnew, B. J., and Patel, G. B. (1997). Structural features of ether lipids in the archaeobacterial thermophiles Pyrococcus furiosus, Methanopyrus kandleri, Methanothermus fervidus, and Sulfolobus acidocaldarius. *Can. J. Microbiol.* 43, 467–476. doi:10.1139/m97-066.

Takai, K., Nakamura, K., Toki, T., Tsunogai, U., Miyazaki, M., Miyazaki, J., et al. (2008). Cell proliferation at 122°C and isotopically heavy CH4 production by a hyperthermophilic methanogen under high-pressure cultivation. *Proc. Natl. Acad. Sci. U. S. A.* 105, 10949–10954. doi:10.1073/pnas.0712334105.

Tayebi, L., Ma, Y., Vashaee, D., Chen, G., Sinha, S. K., and Parikh, A. N. (2012). Long-range interlayer alignment of intralayer domains in stacked lipid bilayers. *Nat. Mater.* 11, 1074–1080. doi:10.1038/nmat3451.

Tornabene, T. G., and Langworthy, T. A. (1979). Diphytanyl and dibiphytanyl glycerol ether lipids of methanogenic archaebacteria. *Science* 203, 51–53. doi:10.1126/science.758677.

Trapp, M., Marion, J., Tehei, M., Demé, B., Gutberlet, T., and Peters, J. (2013). High hydrostatic pressure effects investigated by neutron scattering on lipid multilamellar vesicles. *Phys. Chem. Chem. Phys.* 15, 20951–20956. doi:10.1039/c3cp52762j.

Tristram-Nagle, S. A. (2007). Preparation of Oriented, Fully Hydrated Lipid Samples for Structure Determination Using X-Ray Scattering. *Methods Mol. Biol.* 400, 63–75. doi:10.1007/978-1-59745-519-0_5.

Trovaslet-Leroy, M., Martinez, N., Marion, J., and Peters, J. (2016). "Hautes pressions et dynamique des systems bilogiques," in *Mesures en conditions extrêmes,* ed. Éditions des Archives Contemporaines, 51-64.

Tyler, A. I. I., Law, R. V., and Seddon, J. M. (2015). "X-Ray Diffraction of Lipid Model Membranes," in *Methods in Membrane Lipids* , ed. D. M. Owen (New York, NY: Humana Press), 199–225. doi:10.1007/978-1-4939-1752-5.

Winter, R., and Jeworrek, C. (2009). Effect of pressure on membranes. *Soft Matter* 5, 3157–3173. doi:10.1039/b901690b.

Yamauchi, K., Doi, K., Yoshida, Y., and Kinoshita, M. (1993). Archaebacterial lipids: highly proton-impermeable membranes from 1,2-diphytanyl-sn-glycero-3-phosphocholine. *Biochim. Biophys. Acta* 1146, 178–182. doi:10.1016/0005-2736(93)90353-2.

Yayanos, A. A., Dietz, A. S., and Van Boxtel, R. (1981). Obligately barophilic bacterium from the Mariana Trench. *Proc. Natl. Acad. Sci. U. S. A.* 78, 5212–5215. doi:10.1073/pnas.78.8.5212.

Zeng, X., Birrien, J. L., Fouquet, Y., Cherkashov, G., Jebbar, M., Querellou, J., et al. (2009). Pyrococcus CH1, an obligate piezophilic hyperthermophile: Extending the upper pressure-temperature limits for life. *ISME J.* 3, 873–876. doi:10.1038/ismej.2009.21.

Figure 1. 1D Neutron diffractograms of DoPhPC:DoPhPE (9:1) + 5 mol% h-squalane membrane. **(A)** Diffractograms at 20 bar and temperatures increasing from 25°C to 85°C and after returning to 25°C. Diffraction peaks corresponding to $Phase_{LT}$ are denoted with an 'x' and peaks corresponding to $Phase_{HT}$ are denoted with an 'o'. First order diffraction peaks at 85°C **(B)**, 55°C **(C)** and 25°C **(D)** measured at 20 bar (black), 250 bar (red), 500 bar (blue) and 1000 bar (green).

Figure 2. Coexistence of phases in DoPhPC:DoPhPE (9:1) membrane containing 5 mol% h-squalane. **(A-D)** Plots of peak intensities of $Phase_{LT}$ (blue circles) and $Phase_{HT}$ (green squares) as a function of temperature. Pressures were 20 bar **(A)**, 250 bar **(B)**, 500 bar **(C)** and 1000 bar **(D)**. Error bars are within symbols. **(E)** Pressure-Temperature diagram of the coexistence of $Phase_{LT}$ and $Phase_{HT}$. Error bars indicate standard errors.

Figure 3. (A) + **(B)** Membrane d-spacing as a function of pressure for $Phase_{LT}$ (solid symbols) and $Phase_{HT}$ (open symbols) in DoPhPC:DoPhPE (9:1) membrane containing 5 mol% h-squalane. Temperature was 25 °C (black squares), 40 °C (red circles), 55 °C (blue triangles), 70 °C (green inverted triangles), or 85 °C (purple diamonds). Error for d-spacing measurements is ± 0.5 Å.

Figure 4. Pressure induced swelling of DoPhPC:DoPhPE (9:1) membrane containing different quantities of h-squalane. Swelling of $Phase_{LT}$ containing 2.5 mol% (dark gray), 5 mol% (gray), or 10 mol% (light gray) h-squalane. Swelling of $Phase_{HT}$ containing 2.5 mol% (dark blue), 5 mol% (blue), or 10 mol% (light blue) h-squalane.

584 Table 1: Membrane d-spacing for $Phase_{LT}$ (left table) and $Phase_{HT}$ (right table) for DoPhPC:DoPhPE
585 (9:1) membrane containing h-squalane. N.P.: not present. Error is ± 0.5 Å.

$Phase_{LT}$	+2.5% squalane	+5% squalane	+10% squalane		$Phase_{HT}$	+2.5% squalane	+5% squalane	+10% squalane
25°C 20bar	55.6 Å	55.2 Å	56.0 Å		25°C 20bar	N.P.	N.P.	82.3 Å
25°C 250 bar	56.2 Å	55.5 Å	57.0 Å		25°C 250 bar	N.P.	N.P.	86.7 Å
25°C 500 bar	56.1 Å	55.8 Å	57.1 Å		25°C 500 bar	N.P.	N.P.	88.9 Å
25°C 1000bar	56.2 Å	55.5 Å	57.2 Å		25°C 1000bar	N.P.	N.P.	90.6 Å
40°C 20bar	55.2 Å	54.6 Å	55.7 Å		40°C 20bar	N.P.	70.8 Å	78.6 Å
40°C 250 bar	55.2 Å	54.7 Å	55.8 Å		40°C 250 bar	N.P.	72.2 Å	79.8 Å
40°C 500 bar	55.0 Å	54.7 Å	56.0 Å		40°C 500 bar	N.P.	74.6 Å	82.6 Å
40°C 1000bar	55.6 Å	55.2 Å	56.4 Å		40°C 1000bar	N.P.	76.5 Å	83.6 Å
55°C 20bar	54.1 Å	54.0 Å	55.3 Å		55°C 20bar	67.1 Å	68.1 Å	74.7 Å
55°C 250 bar	54.8 Å	54.0 Å	55.7 Å		55°C 250 bar	68.5 Å	69.3 Å	75.9 Å
55°C 500 bar	55.2 Å	54.3 Å	55.3 Å		55°C 500 bar	69.4 Å	70.6 Å	77.3 Å
55°C 1000bar	55.2 Å	54.4 Å	56.1 Å		55°C 1000bar	72.2 Å	73.7 Å	80.0 Å
70°C 20bar	53.8 Å	53.5 Å	54.4 Å		70°C 20bar	65.7 Å	66.8 Å	72.4 Å
70°C 250 bar	54.0 Å	53.9 Å	55.3 Å		70°C 250 bar	65.7 Å	67.5 Å	74.3 Å
70°C 500 bar	54.2 Å	53.9 Å	55.2 Å		70°C 500 bar	67.7 Å	68.2 Å	74.1 Å
70°C 1000bar	54.8 Å	53.7 Å	55.2 Å		70°C 1000bar	70.1 Å	70.6 Å	75.3 Å
85°C 20bar	53.5 Å	53.6 Å	N.P.		85°C 20bar	64.9 Å	65.0 Å	74.1 Å
85°C 250 bar	53.5 Å	53.6 Å	54.3 Å		85°C 250 bar	65.4 Å	65.9 Å	75.4 Å
85°C 500 bar	53.6 Å	53.9 Å	54.5 Å		85°C 500 bar	65.9 Å	66.4 Å	74.8 Å
85°C 1000bar	53.7 Å	54.0 Å	54.8 Å		85°C 1000bar	67.3 Å	67.6 Å	76.3 Å

586

587 Table 2: Temperature at which $Phase_{HT}$ appears in DoPhPC:DoPhPE (9:1) membrane containing h-
588 squalane.

Pressure	2.5% squalane	5% squalane	10% squalane
20 bar	44.7 ± 4.0 °C	34.3 ± 3.9 °C	23.9 ± 3.4 °C
250 bar	49.3 ± 1.5 °C	37.4 ± 3.2 °C	28.8 ± 3.3 °C
500 bar	49.2 ± 0.1 °C	37.7 ± 3.0 °C	31.8 ± 1.6 °C
1000 bar	50.8 ± 1.2 °C	38.9 ± 2.6 °C	32.2 ± 2.6 °C

589

Figure 1.TIF

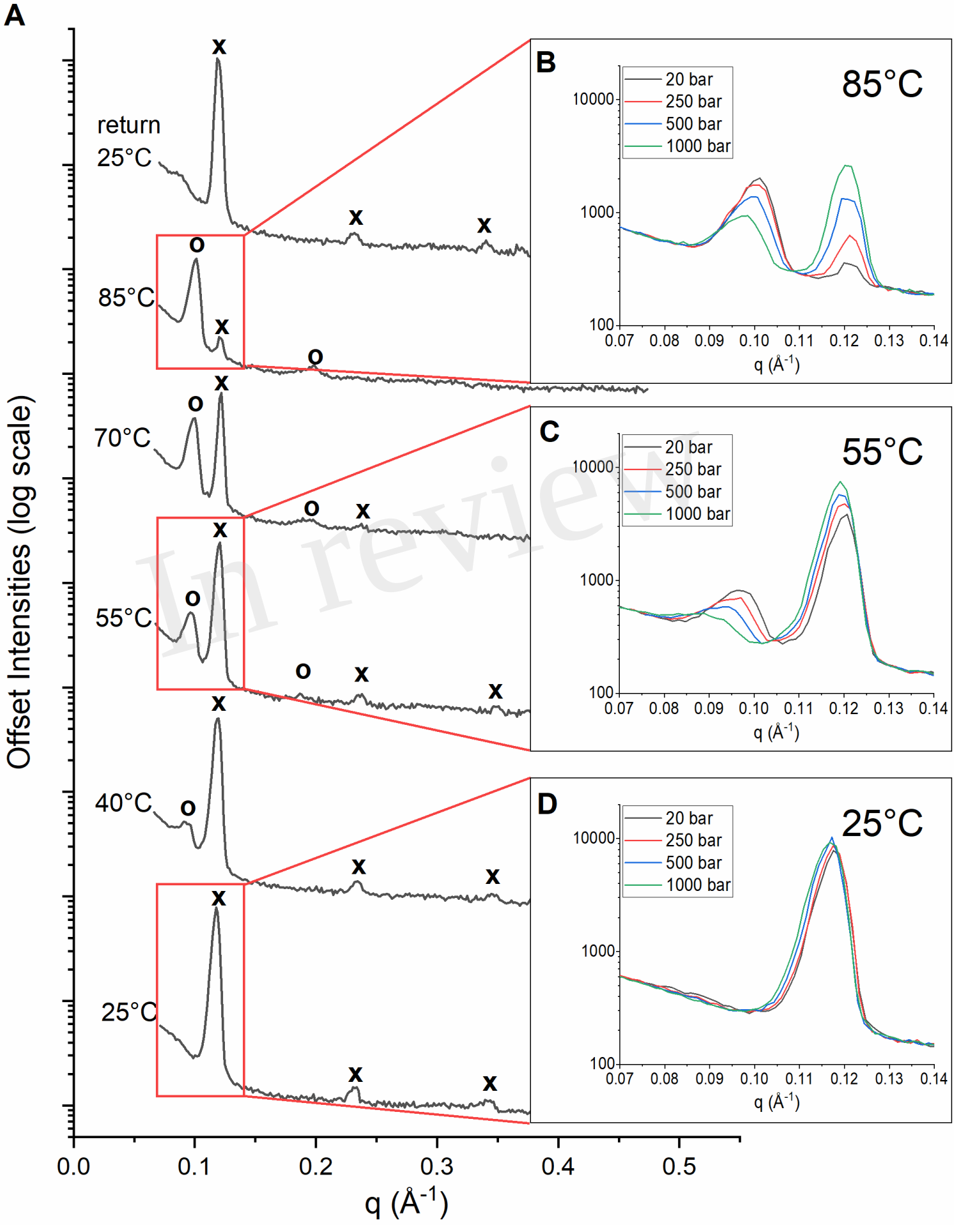
A
B
C
D
return
25°C
85°C
70°C
55°C
40°C
25°C
x
o
Offset Intensities (log scale)
q (Å-1)
0.0
0.1
0.2
0.3
0.4
0.5
20 bar
250 bar
500 bar
1000 bar
85°C
55°C
25°C
10000
1000
100
0.07
0.08
0.09
0.10
0.11
0.12
0.13
0.14
In review

Figure 2.TIF

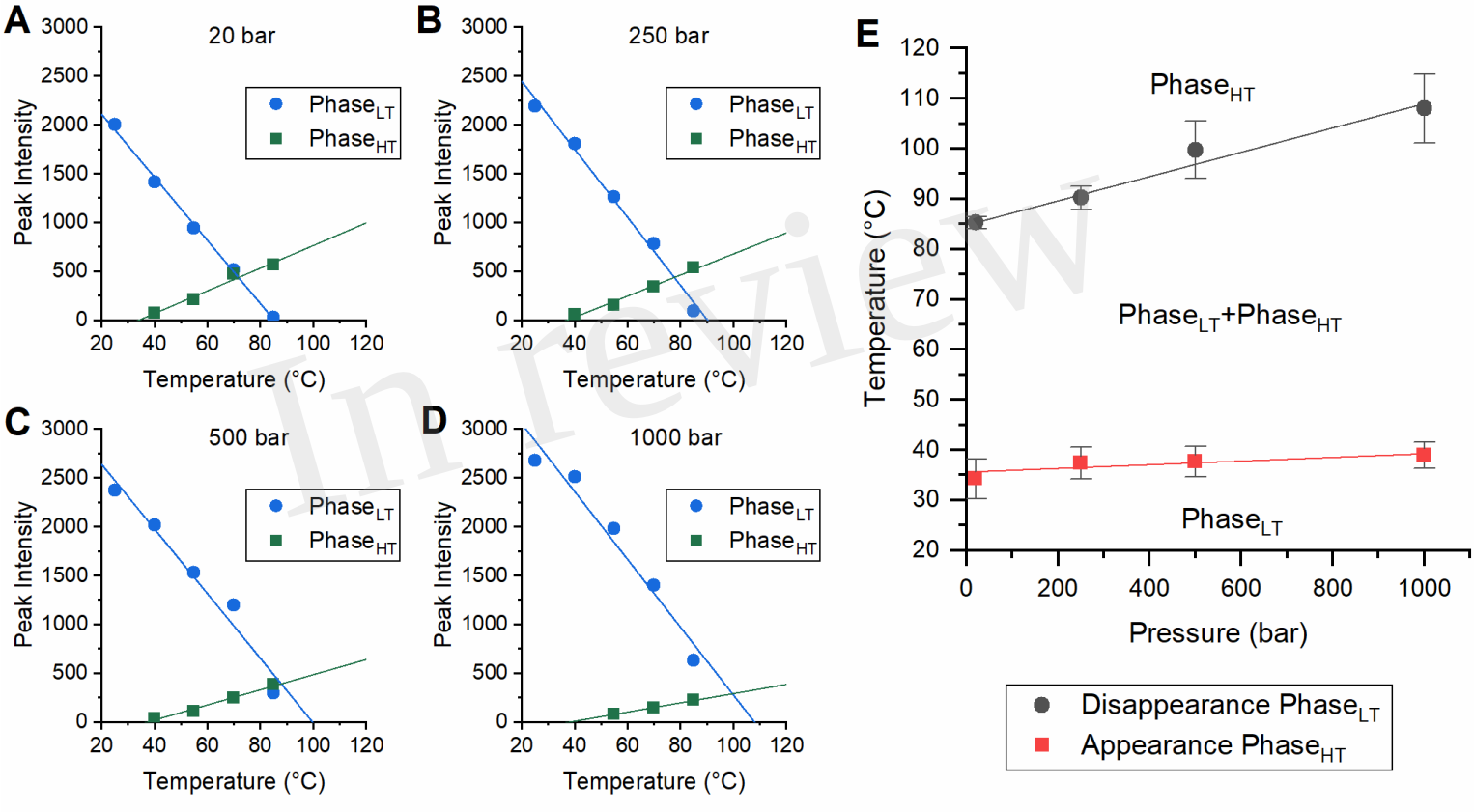

Figure 3.TIF

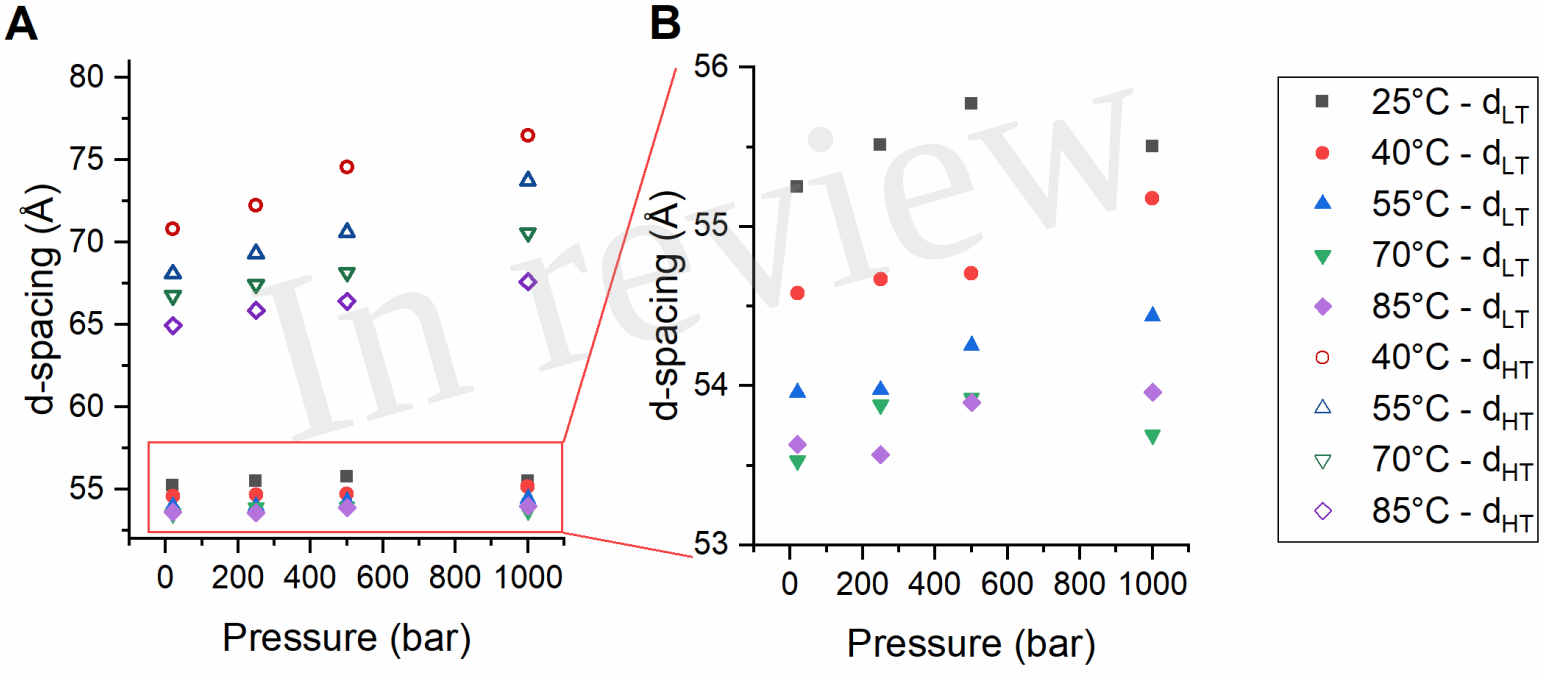

Figure 4.TIF